J. Fluid Mech. (1974), *vol.* 65, *part* 3, *pp.* 499–512
Printed in Great Britain

Anomalous drag-reducing phenomenon at a water/fish-mucus or polymer interface

By S. C. LING

Department of Aerospace and Atmospheric Sciences, The Catholic University of America, Washington DC 20017

AND T. Y. J. LING

Department of Zoology, University of Maryland, College Park, Maryland 20742

(Received 30 August 1973 and in revised form 28 January 1974)

The sublayer of a turbulent boundary-layer flow with and without polymer additives was measured by a simple optical technique having a high degree of spatial resolution. The reduction of skin friction with polymer additives was found to be due to a decrease in the effective viscosity of water at the interface between the mucus (glycoprotein) or polymer (polyethylene oxide) and the water and a thickening of the laminar sublayer. The rate at which mucus diffuses away from a medium-sized fish is almost constant for all swimming speeds.

1. Introduction

Although the effect of drag reduction due to dilute polymer solutions has been subjected to intensive investigation (Rudd 1969; Van Driest 1970; Virk 1971; see also the extensive survey by Hoyt 1972), the exact mechanism responsible for the phenomenon is still uncertain. This is due in part to the lack of a precise technique for probing the sublayer flow. It is therefore the objective of this paper to present a technique through which some of the basic mechanisms responsible for the reduction in skin friction can be identified. In contrast to the case where the entire fluid is a homogeneous solution of polymer, the present study is limited to the case where there is a distinct layer of mucus or polymer over the flow boundary. The former case has been studied in many investigations, which include all the references cited above.

The coatings of mucus (long-chain glycoprotein molecules) over the bodies of fish and on the inner surfaces of blood vessels and moving joints are some of the important occurrences of natural lubricants. Early interest in this subject may be found in the work of Jakowska (1963) and Rosen & Cornford (1971). As a first step towards understanding and studying the physical properties of mucus, one must devise some means through which both the distribution of shear stress and the velocity field can be measured within the tenuous laminar sublayer. A simple optical technique with a spatial resolution of $15\,\mu$m was developed through the use of the shallow focal depth of a microscope in conjunction with

selective illumination of its objective plane by a focused laser beam. Microscopic trace particles (illuminated by the beam) traversing the objective plane were detected photoelectrically and indicated the local velocity. A preliminary investigation of this method was reported by Aquino & Lamontagne (1973). More advanced details of this technique are discussed in § 2. With this method an anomalous drag-reducing layer was observed in both turbulent and laminar boundary-layer flows. For example, the anomalous flow phenomena found over the bodies of small fish and in blood vessels are unsteady but laminar, while those over the bodies of large fish, ships and pipes are turbulent.

The viscoelastic properties of a non-Newtonian fluid are generally expressed as functions of the strain invariants (Fredrickson 1964). A complete determination of the physical properties of low viscosity fluids, such as dilute solutions of mucus and polymer, under high shear stress is at present an unsurmountable task. This is because such a fluid tends to become turbulent at high shear stress. The problem may be overcome by considering a small-scale version of the flow field, but this introduces additional problems which impede accurate measurements. However, this technique is still being investigated. In the meantime, the best one can do when studying the drag-reducing phenomenon is to measure both the mean velocity gradient and shear stress within the turbulent boundary layer and to observe the behaviour of the effective or apparent kinematic viscosity defined as

$$\nu_i = \frac{\tau_{yz}}{\rho \partial U_z/\partial y}, \tag{1}$$

where τ_{yz} is the mean shear stress on a fluid element, ρ the mass density of the fluid and $\partial U_z/\partial y$ the mean velocity gradient within the fluid element. For a turbulent non-Newtonian flow field, the effective viscosity should not be simply taken as a material property of the fluid, because it is composed of both eddy viscosity and molecular viscosity, which are in turn functions of the rate of strain. However, by studying the behaviour of the effective viscosity over a wide range of shear stresses and polymer concentrations, one may be able to make some inferences about the physical properties of the mucus. Experimental results, for wall shears ranging from 10 to 500 dyn/cm^2, showed the existence of an anomalous flow layer sandwiched between the laminar sublayer and the turbulent transition layer. The effective viscosity within the anomalous layer was found to be less than that of water. Whether the anomalous effect is due to shear thinning of the molecular viscosity or the existence of a negative eddy viscosity, or both, is at present uncertain.

2. Method

A fully developed turbulent pipe flow is considered to be the simplest flow field one can use to study the drag-reducing phenomenon for mucus. Under such conditions the flow profile $U(y)$ remains essentially constant and steady in the flow direction z, and the distribution of the shear stress τ_{yz} can be related to the pressure gradient $\partial p/\partial z$ along the pipe (Schlichting 1968, p. 560) by

$$\tau_{yz} = \tfrac{1}{2}(y-R)\,\partial p/\partial z,$$

where y is the radial distance from the wall of the pipe and R is the inner radius of the pipe. Thus τ_{xz} decreases with y, and the shear stress τ_0 at the wall is

$$\tau_0 = -\tfrac{1}{2}R\,\partial p/\partial z. \tag{2}$$

When the sublayer is thin with respect to R, one may assume the shear stress to be nearly constant within this layer and approximately equal to τ_0. Using the mean velocity gradient calculated from the measured velocity profile, the effective kinematic viscosity within the flow field can be evaluated through (1). If the ratio ν_i/ν_w of the effective kinematic viscosity of the polymer–water solution to the kinematic viscosity of water is found to be less than unity, it will temporarily be defined as an anomalous kinematic viscosity; since the mechanics responsible for such physical behaviour are still unknown. For values much greater than unity, ν_i is dominated by the conventional kinematic eddy viscosity.

2.1. *Experimental set-up*

The experimental set-up for studying the friction reduction effect of both natural mucus and polyethylene oxide is shown in figure 1. It consists of a recirculating water system maintained by a standard sump pump. Dechlorinated tap water was pumped from a large holding tank through a flowmeter which was calibrated to an accuracy of $\pm 1\,\%$. This meter served to monitor the flow during an experiment as well as to verify the flow rate obtained from the measured flow profile. The flowmeter outlet was connected to the inlet of the test section. The test section was a 1·27 cm I.D. clear lexan tube 2 m long with a 3·2 mm wall. The main reason for not using a larger pipe was the limited amount of mucus available for performing the experiment; also the 1·27 cm pipe was considered to be sufficiently large so that at high wall shears the sublayer thickness was small compared with the pipe radius. Under these conditions, the effect of the pipe radius may be negligible. To facilitate changing and cleaning the system, the test section was made of several sections of tube connected together by quickly disconnecting collars. To avoid the need for an excessively long test section to achieve a fully developed turbulent flow, a flow straightening section made of packaged drinking straws 3 cm long was used in place of the usual inlet contraction. Following the flow straightener was a polymer injection station which consisted of a series of 0·06 cm holes drilled through the test section, with the holes making a 30° angle with respect to the wall. There were two rings of holes with 20 holes per ring. The holes in each ring were staggered. Thus, a uniform layer of polymer solution could be injected over the inner surface of the test section. A similar polymer injector system using porous tubes has been described by Walters & Wells (1971). The distribution chamber over the drilled holes was connected to a polymer-solution storage bottle hung 5 m above the test section. Polymer solution of different concentrations could then be fed by gravity into the test section and regulated by a control valve on the feed line. Following the polymer injector was a test section 1 m or 80 pipe diameters long which was used for establishing a fully developed turbulent flow. After this section was a second polymer injector similar to the first for the purpose of compensating for the loss

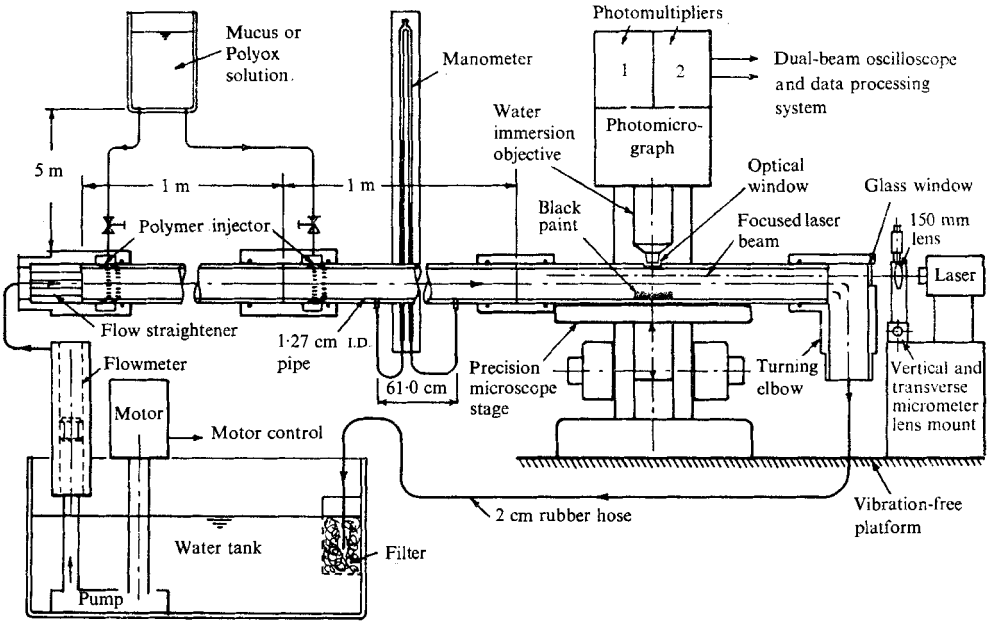

FIGURE 1. Experimental set-up.

of polymer solution by diffusion into the main flow. Following the second injector station was a 1 m long test section which was used for monitoring the pressure gradient along the tube. Two pressure taps, 61·0 cm apart, were installed on this test section. The taps were connected to a manometer as shown in figure 1. Following this section was the microscope and laser light station where the flow profiles were measured. This part of the test section was approximately 12 cm long and was cast onto a base plate which in turn was bolted onto the precision moving stage of the microscope. The stage was of the type which could be set and read to within $\pm 1\,\mu$m. An optical window on top of the test section was provided directly below the objective of the microscope. The window was made by milling a precisely flat surface which was both normal to the optical axis of the microscope and tangential to the inner surface of the test section. This opening was covered with a 0·12 mm thick cover glass which was mounted with care to ensure that it was flat and that the inner surface of the test section was smooth. To avoid stray illumination in the glass, opaque epoxy cement was used for mounting the cover glass. To provide a dark field for the microscope, the inner surface of the tube directly below the glass window was sprayed with non-reflecting black paint. Located at the end of the test section was a quickly disconnecting elbow which had two internal guide vanes for directing the flow efficiently around the elbow and back into the holding tank. As indicated in figure 1, a 15 mW laser light was mounted on an adjustable platform so that the beam could be directed through a second glass window placed at the top vertical edge of the elbow. The beam was first approximately aligned along the axis of the test section and centred with respect to the objective plane of the microscope. The 0·8 mm laser beam was further focused to a diameter of approximately $15\,\mu$m by a simple lens

with a focal length of 150 mm. The lens was mounted on a two-axis micrometer stage to facilitate fine vertical and lateral adjustments of the focused beam to the exact centre of the objective plane. Because all optical systems were mounted on a solid and vibration-free platform, we note from figure 1 that, as the microscope stage is raised or lowered, the laser beam will traverse the flow field but will not move with respect to the objective plane of the microscope. With this technique any microscopic region of the flow field can be selectively examined and studied. The microscope was further equipped with a photomicrographic attachment so that a mask with two narrow slits could be placed in the film plane of the micrograph. The slits were 0·3 mm wide by 5 mm long and spaced in parallel 2·54 cm centre to centre. The two slits were also oriented normal to the direction of the flow, so that the transit time for the image of an illuminated trace particle moving from the first slit to the second slit could be detected and measured. In focusing this optical system one should use only the eye-piece provided for focusing the photomicrograph. Reference data for the flow field were obtained by focusing the micrograph on some minute dirt particle on the inner surface of the cover-glass window. For better accuracy, the optical gain for the micrograph was precalibrated for each of the objectives used. Two photomultiplier tubes, senstive to the red spectrum, were enclosed and placed one over each slit. The signals from the photomultipliers were amplified and fed into a dual-beam oscilloscope equipped with a precision time base. Both oscilloscope beams were triggered by the signal pulse from the first slit. Hence the delay time of the signal pulse from the second slit relative to that of the first slit could be read off from the calibrated screen of the oscilloscope or by a digital time interval counter. Only signals with sharp spikes free of extraneous pulses were sampled. Several hundred readings, with the actual sample size depending on the standard deviation of the data (or intensity of turbulence), were averaged to obtain the mean delay time t. Thus, the mean velocity U of the flow can be expressed simply as

$$U = S/G_x t, \tag{3}$$

where S is the spacing of the slits and G_x is the calibrated optical gain of the micrograph.

All the experiments were conducted within a temperature range of 19–28 °C. The exact temperature of the water was monitored for each experimental measurement, and the effect of the temperature was reflected in the kinematic viscosity ν_w of water used to normalize the measured data.

2.2. *Preparation of fish mucus for tests*

The main criterion in our search for species of fish to be used in the present study was the available quantity rather than the quality of external fish mucus. Mucus from several species of fish found locally in the Chesapeake Bay area was considered.

The bodies of the catfish (*Ictalurus catus*) and the eel (*Anguilla rostrata*) are coated with mucus that shows a high reluctance to diffuse in water and a tendency to form insoluble clumps when removed from the skin, thus rendering it impossible to use in this study. The white perch (*Morone americana*) and the

striped bass (*Roccus saxatilis*), which are also commonly found in the bay area, have mucus showing good friction reduction properties; however, the quantity of mucus we were able to obtain from these fish was too limited for conducting extensive velocity profile measurements. The small flatfish (*Trinectes maculatus*) locally known as the hogchoker (figure 2, plate 1) was found to have the ability to secrete large quantities of mucus. The hogchoker, in its natural habitat, spends much of its time on muddy substrata, but has been observed to swim with fast bursts of speed when disturbed or excited. The fish propels itself by making a travelling wave motion with both its dorsal and ventral fins, as well as its body and tail. Because the reduction of friction by mucus over the body of a fish is a complex boundary-layer problem, beyond the scope of this paper, our present aim was to find a way to extract the mucus and study it in a less complicated flow field. The mucus was obtained by piling the fish into a shallow bucket filled with a known quantity of water sufficient to keep them wet but not covered. By gently rocking the bucket for 10–20 min a sizeable quantity of concentrated mucus was secreted. This process can be repeated several times for each batch of hogchokers. Following the mucus extraction process the fish were returned to the bay. It will be shown in the following section that the physical properties of hogchoker mucus are very similar to those of the water/polyethylene oxide solution Polyox WSR-301, produced by Union Carbide. Because of this similarity, a water solution of Polyox 301 was used to obtain detailed measurements of the flow profiles, while the limited supply of hogchoker mucus was used to verify, under similar flow conditions, a few critical points on the flow profiles. In the course of our study, we have observed that both fish mucus and Polyox 301 are extremely sensitive to degradation by chlorine found in ordinary tap water. Thus distilled water was used to dissolve the dry polyethylene oxide powder and bay water to dilute the hogchoker mucus.

In order to obtain some information concerning the natural concentration of mucus, a known volume and weight of hogchoker mucus was washed with distilled water in a filter system until the mucus was salt free. The mucus material retained on the filter was then dried at 60° C for seven days in an oven and then weighed. From this dry weight the concentration of hogchoker mucus was found to be approximately 2000 p.p.m. by weight.

3. Results and discussion

Fish mucus is secreted by cells of the epidermis which form glands that lead to the surface of the fish through ducts and pores. Water flowing over the surface will then spread the mucus evenly downstream while a small amount diffuses into the outer flow field. Thus by injecting the concentrated polymer into the inner surface of the test section as described in § 2, one can simulate the coating of mucus over the body of the fish. Because the diffusion of polymer normal to the flow is small, the polymer layer is convected a long distance downstream before losing its effectiveness. Therefore, in the following studies of the sublayer profiles, neither the diffusion nor distribution of mucus was taken as a major controlling parameter; but they will be treated in a separate study.

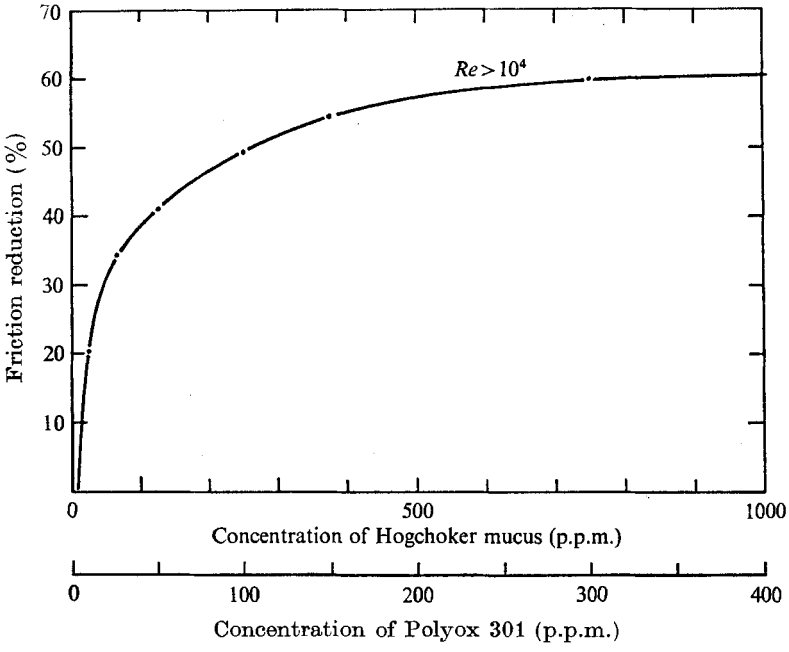

FIGURE 3. Percentage friction reduction as function of the concentration of hogchoker mucus and Polyox 301 for $Re > 10^4$.

The sublayer profile should be a function of the polymer concentration, apparent kinematic viscosity of the polymer solution, wall shear and the Reynolds number of the pipe flow. To find their functional relationship we chose to run the experiment at five fixed Reynolds numbers $Re = 5500$, 11600, 18800, 47000 and 74000, where Re is based on the mean discharge velocity $\overline{U}$ of the pipe, the pipe diameter D and the kinematic viscosity ν_w of water. For each Re, flow profiles were measured for polymer concentrations of 0, 50 p.p.m. and > 500 p.p.m. of Polyox 301; and 120 p.p.m. (6 %) and > 1500 p.p.m. (75 %) of hogchoker mucus. These concentrations were chosen for their practical importance. Measurements for the pure-water case were made to serve as an experimental check and to provide reference data for the other measurements. The cases with 50 p.p.m. of Polyox 301 and 120 p.p.m. of hogchoker mucus were chosen to produce a similar 40 % reduction in wall shear without a significant increase in the sublayer thickness with respect to the pure-water case. The cases with > 500 p.p.m. of Polyox 301 and > 1500 p.p.m. of hogchoker mucus were chosen to represent flow in the natural state, which was characterized by a thick sublayer and a 60 % reduction in wall shear. A plot showing the effect of polymer concentration *vs.* percentage of shear reduction with respect to the pure-water case at similar Re is shown in figure 3. The plot indicates that there is a saturation level at which further increases in polymer concentration will not lead to further reductions in wall shear. For example, at shear reductions greater than 40 % increases in the polymer concentration result in only slight increases in shear reduction; while for shear reductions below 40 % the function decreases rapidly

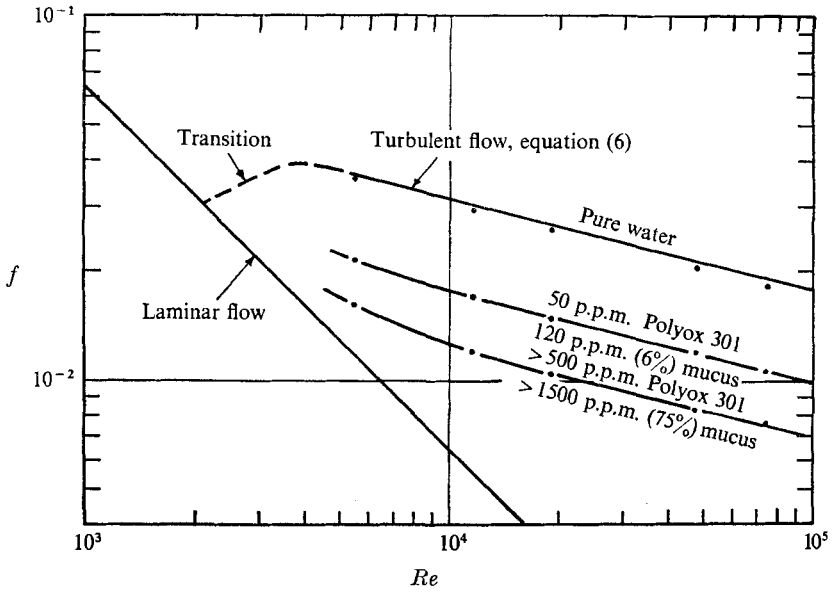

FIGURE 4. Coefficient of friction as a function of pipe Reynolds number for different concentrations of hogchoker mucus and Polyox 301 within the sublayer.

with a reduction in polymer concentration. The plot also shows that for $Re > 10^4$ the percentage of shear-stress reduction is independent of Re. At lower Re the efficiency of shear reduction is lowered (not shown).

It is convenient to express the wall friction or shear in terms of the usual friction factor f for pipe flow defined as follows (Schlichting 1968, p. 561):

$$-\partial p/\partial z = f\rho\overline{U}^2/2D, \tag{4}$$

where f is a function of both Re and the concentration of polymer.

Substituting (2) into (4) we write

$$\tau_0 = \tfrac{1}{8}f\rho\overline{U}^2.$$

Thus,
$$f = 8\tau_0/\rho\overline{U}^2 = 8U^{*2}/\overline{U}^2, \tag{5}$$

where $U^* = (\tau_0/\rho)^{\frac{1}{2}}$ is the shear velocity. The measured friction factor f is plotted in figure 4 for pure water, concentrations of 50 p.p.m. and > 500 p.p.m. of Polyox 301 and the corresponding values for hogchoker mucus. The pure-water line represents the friction factor for the case of turbulent flow in a smooth pipe given by Prandtl (Schlichting 1968, p. 574) as

$$f^{-\frac{1}{2}} = 2{\cdot}0\log(Ref^{\frac{1}{2}}) - 0{\cdot}8. \tag{6}$$

The data points obtained from our experimental set-up fall slightly below this line. The line with a $-45°$ slope on the left side of figure 4 is the friction-factor line for laminar flow. Note that for the case of low polymer concentration the data curve is parallel to but shifted down by approximately 40% from the pure-water case, except for points with $Re < 10^4$. Similarly for the case of concentrated polymer the data line is parallel but shifted down by 60%. For $Re < 10^4$ the percentage of friction reduction is smaller and the lines tend to merge into the laminar line. Hence, the threshold for efficient shear reduction occurs at $Re > 10^4$.

In contrast to the present study, Virk (1971) reported, for the case in which the whole field contained a uniform concentration of polymer, that there was a maximum friction reduction asymptote which when plotted in figure 4 would fall between the friction-factor lines for the laminar flow and the present data. Under these conditions, flow within the pipe was no longer fully turbulent. Even so, this effect was unexplainable unless there was a substantial reduction in the effective viscosity within the sublayer. It should be noted that the f factor defined by (4) is four times larger than the f factor used by Virk (1971).

For all cases except one, the lateral diffusion of mucus or Polyox 301 solution into the flow field was small within the 2 m long test section, such that additional injection of polymer by the second polymer injector (see figure 1) produced no extra reduction in friction. The only exception was for the case with $Re = 74\,000$, in which an additional injection of polymer at the second injection station was required in order to maintain a maximum of 60 % friction reduction. This indicated that the lateral diffusion of polymer was high owing to intense turbulence and wall shear; hence, polymer had to be injected at shorter intervals in order to make up for the loss through diffusion. It should be noted that all the cases of low polymer concentration could also be obtained with polymer solution of high concentration by simply reducing the injection rate until the same percentage of friction reduction was achieved; i.e. when the injected flow rate of the concentrated polymer solution was much less than the flow rate of the laminar sublayer, the polymer would diffuse to a lower concentration within the sublayer. This was in contrast to the above cases in which the injection of polymer was increased until a maximum reduction of friction for the given concentration was achieved. The optimum rate was found to be approximately 40 % of the laminar sublayer flow rate. At this rate the concentration of mucus near the flow boundary could be maintained close to that of the initial injection. Extra solution injected would be lost quickly into the turbulent flow field with no useful effect. Both the diffusion and distribution of the mucus within the sublayer should be analogous to the diffusion from a heat source within a shear field (Ling 1963).

It was found that the flow profiles of dilute polymer solutions have self-similar forms when normalized by the wall shear, i.e., the mean velocity $U(y)$ is normalized by the shear velocity U^* as $U^+ = U/U^*$, and the normal distance y from the wall is normalized by both the shear velocity U^* and the kinematic viscosity ν_w of water as $y^+ = yU^*/\nu_w$.

Profiles for the three polymer concentrations, i.e. zero, low and high concentration, are shown on a semi-log plot in figure 5. For each polymer concentration there are five profiles, corresponding to the five different Reynolds numbers mentioned earlier. The lowest curve, with open symbols representing the five different Reynolds numbers, is for pure water. This curve is the universal turbulent flow profile for Newtonian fluid. For the case of low polymer concentration, 50 p.p.m. Polyox 301 and 120 p.p.m. hogchoker mucus, the flow profiles corresponding to the five different Reynolds numbers are shown as the curve with crosses and V symbols. We note that all five profiles also have a self-similar form. For the case of high polymer concentration, > 500 p.p.m. Polyox 301 and > 1500 p.p.m. hogchoker mucus, the flow profiles corresponding to the same five Reynolds

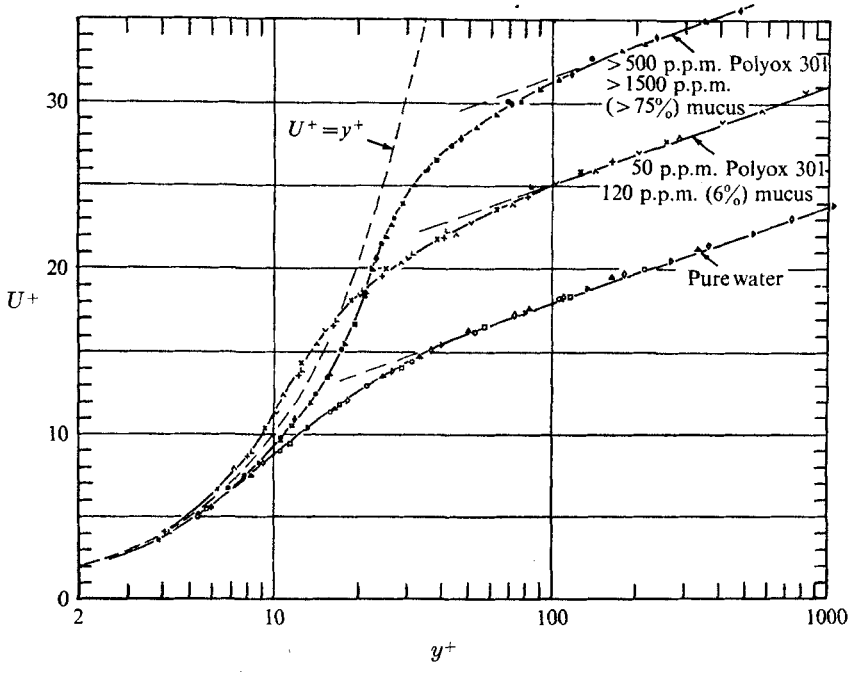

FIGURE 5. Semi-log plot of normalized velocity profiles for different concentrations of hogchoker mucus and Polyox 301 within the sublayer.

	◣	◆	▲	●	■
	V	^	×	+	L
	▷	◇	△	○	□
Re	74000	47000	18800	11600	5500

numbers are shown as solid symbols. Here again, all five profiles have a self-similar form. We note that all three cases have similar (logarithmic) turbulent flow profiles represented by the straight lines with equal slopes. This means that the distribution of eddy viscosity in these layers is the same. The only difference is that their spatial locations are dictated by different sublayer structures, and they are noted to be located approximately at y^+ above 40, 100 and 110, respectively, for the three cases cited. The basic feature of this layer is in agreement with most published data; i.e. it is independent of the polymeric parameters. Because our interest was in the sublayer structure, the regular wake layer representing the flow in the central core of pipe was not presented.

To study the sublayer structure, it is more instructive to plot the sublayer profiles on a linear plot as shown in figure 6. Here y^+ was plotted as the ordinate and U^+ as the abscissa. The laminar profile $y^+ = U^+$ was also plotted as the dashed reference line. The same symbols were used to label the three sets of profiles. The curves that best fitted the data points were drawn. From these curves one can obtain the effective kinematic viscosity through (1), after normalizing the variables in the equation, as

$$\frac{\nu_i}{\nu_w} = \frac{\tau_{yz}}{\tau_0}\left(\frac{\partial U^+}{\partial y^+}\right)^{-1}. \tag{7}$$

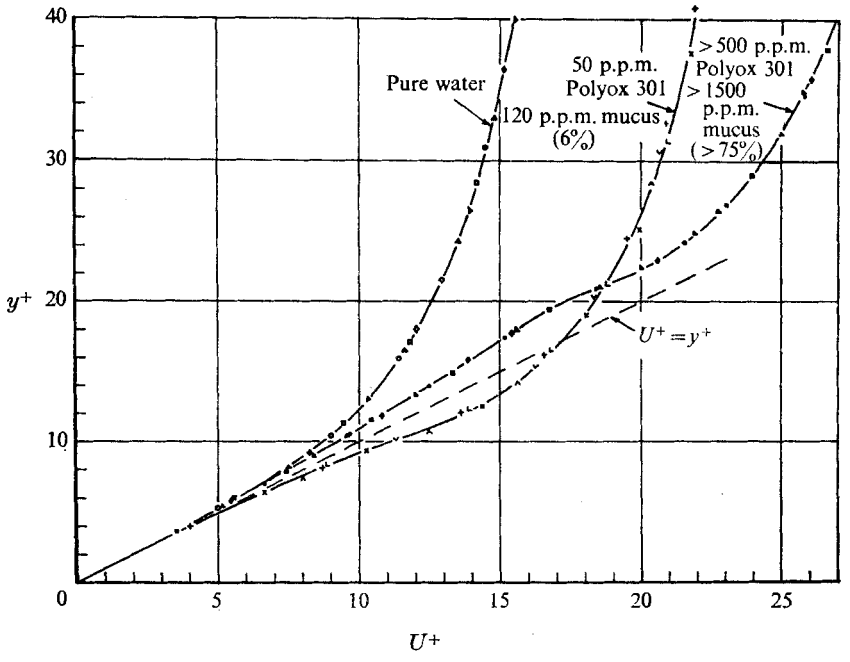

FIGURE 6. Linear plot of normalized sublayer profiles for different concentrations of hogchoker mucus and Polyox 301 within the sublayer.

This states that the ratio of the effective kinematic viscosity of the flow to the kinematic viscosity of water is the reciprocal of the velocity gradient of the normalized flow profile, if τ_{yz}/τ_0 is taken to be approximately unity within the tenuous laminar sublayer. The result is plotted in figure 7.

For the Newtonian case (zero concentration), we note that the actual laminar sublayer is extremely thin as indicated by the effective viscosity plot in figure 7. In the transition layer $y^+ = 5$–40, the effective viscosity does not increase linearly with y^+. This is verified by the data of both Schubauer and Laufer (Hinze 1959, p. 527). For the case of a low concentration of polymer, 50 p.p.m. Polyox 301 or 120 p.p.m. hogochoker mucus, the laminar sublayer is also very thin. For $y^+ = 8$–12, an anomalous layer with an approximately 40 % increase in velocity gradient is clearly depicted in figure 6. The corresponding distribution of the effective viscosity in this layer is shown in figure 7. It is less than the apparent viscosity ratio of 1·09 for the dilute mucus near zero shear, thus indicating a shear thinning in the laminar sublayer and a large reduction in the effective viscosity in the anomalous flow layer. We note that the anomalous reduction in viscosity is responsible for the observed decrease in shear, since for this case there is no substantial increase in the thickness of the laminar sublayer. For the case of a high concentration of polymer, > 500 p.p.m. Polyox 301 or > 1500 p.p.m. hogchoker mucus, we note that within the thick laminar sublayer the effective viscosity ratio is approximately 1·2 while the apparent viscosity ratio near zero shear is 1·9. Above this layer there is a distinct anomalous flow layer between $y^+ = 19$ and 23. This is seen more clearly in the linear plot than in the semi-log

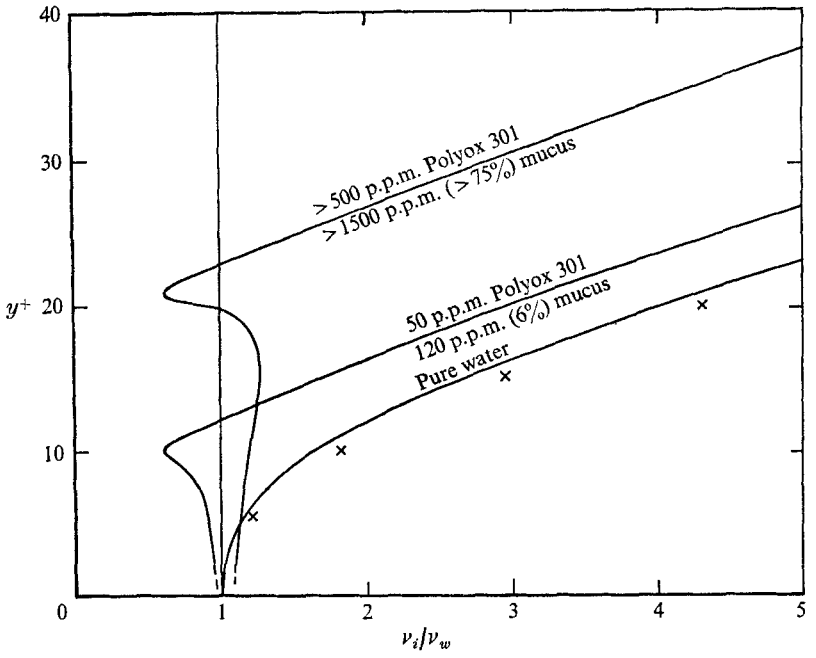

FIGURE 7. Distribution of effective kinematic viscosity within the sublayer for different concentrations of hogchoker mucus and Polyox 301. ×, data from Schubauer and Laufer (Hinze 1959).

plot. Here, again, we observe a similar anomalous reduction in the effective kinematic viscosity. The anomalous flow layer was also found to be the zone of maximum turbulence. From this, it is postulated that both the turbulent shear stress as well as the mean shear stress acting on the nonlinear and non-isotropic properties of the mucus or polymer are responsible for the anomalous flow. For the present problem one may consider the anomalous flow layer as an intermediate layer between the layer of polymer solution and the ambient water, because outside this layer the concentration of the polymer will be greatly diluted by the diffusivity of the turbulent field. We note that not only the anomalous flow layer but also the transition layer for the concentrated polymer case is nearly identical to that for the low concentration case. This is indicated by an identical thickness for the transition layer, $\Delta y^+ \simeq 88$, and an almost constant increase in the effective kinematic viscosity with y^+. The only difference is that these layers are located at different heights controlled by the laminar sublayer. From these results, it is evident that the fully turbulent layer, the transition layer and the anomalous flow layer are independent of both Re (for $Re = 10^4$–10^5) and polymer concentration (for > 50 p.p.m. Polyox 301 and > 120 p.p.m. hogchoker mucus). Friction reduction for the concentrated polymer case is seen to be partly due to the anomalous flow layer and partly due to the thickening of the laminar sublayer. The existence of a thick laminar layer may be explained by the combined effect of a higher apparent viscosity for the sublayer and the presence of an anomalous layer. Thus to optimize the friction reduction effect, one would

maximize both the anomalous flow effect and the sublayer thickness, and minimize the rate of diffusion of the polymer solution from the laminar sublayer.

It would be of interest to relate our turbulent profile data to those for a swimming fish. If we assume that the mean surface friction of a fish swimming at a speed of 1 m/s is equivalent to a turbulent pipe flow having the same centre-line velocity in a 1·27 cm diameter pipe, it will have a wall shear of 8 dyn/cm^2 and a laminar sublayer of concentrated mucus approximately 0·5 mm thick. When swimming at a speed of 5 m/s the fish will have a wall shear of approximately 170 dyn/cm^2 and a laminar sublayer of mucus reduced to a thickness of 0·13 mm. Without a mucus coat, the fish would have a wall shear 2·5 times greater than when covered by mucus. From the present result, it can be shown that, owing to the thinning of the laminar (mucus) sublayer with an increase in swimming speed, the diffusion rate of mucus from a fish is almost constant within a wide range of swimming speeds. That is, if the fish is less than 2 m long and swimming at between 1 and 5 m/s, one may neglect the lateral diffusion of mucus and calculate the convective flow rate q_m of mucus as

$$q_m/W \simeq \tfrac{1}{2}KU_s y_s = \tfrac{1}{2}K\nu_w U_s^+ y_s^+ = 60\nu_w, \tag{8}$$

where W is the mean circumference of the fish body, $K = 0{\cdot}4$ is a correction factor for the distribution of mucus concentration within the laminar sublayer and U_s is the convective velocity at the top y_s of the laminar sublayer. Since q_m depends only on W, a fish with a large length-to-width ratio will make more efficient use of its mucus.

4. Conclusion

We have demonstrated that the sublayer velocity field can be measured with a significant degree of resolution through selective illumination of the objective plane of a microscope with a finely focused laser beam. With this technique any microscopic flow field can be readily measured and studied. So far we have seen that the sublayer velocity field of a swimming fish consists of three distinct layers.

(i) A laminar sublayer of concentrated mucus or polymer solution whose apparent viscosity and thickness are dependent on the polymer concentration.

(ii) A thin anomalous flow layer in which the effective viscosity is less than that of the solvent and independent of the polymer concentration within the laminar sublayer. Further work must be conducted to define both the turbulent field and the polymeric parameters before one can understand the mechanics of the anomalous phenomenon.

(iii) A transition flow layer in which the eddy viscosity increases almost linearly with the distance from the boundary. Its thickness is also independent of the polymer concentration within the laminar sublayer.

All these layers exhibit self-similar forms when normalized by the wall shear.

Before one can handle the overall problem of the frictional drag on a swimming fish, further studies must be conducted on the development of laminar flow

involving the anomalous flow effect. Nonetheless, it is clearly evident that the mucus covering the body of the fish serves to reduce frictional drag in addition to functioning as a biological defence mechanism against micro-organisms and other possible contaminants.

We wish to express our deep gratitude to Dr T. S. Y. Koo, Chairman of the Department of Fisheries, Chesapeake Biological Laboratory, Solomon Island, Maryland, Dr M. L. Wiley, Mr R. E. Miller and Mr D. E. Ritchie for their generous hospitality, advice and assistance while this work was being performed at the Chesapeake Biological Laboratory; also to Dr H. B. Atabek and Dr C. Rees for their helpful suggestions. This work was conducted under the support of U.S. Public Health Service Grant HE 12083-05 and National Aeronautical and Space Administration Grant NGL 09-055-067.

REFERENCES

AQUINO, H. & LAMONTAGNE, R. 1973 *A.I.A.A. 9th Ann. Meeting*, paper 73–39.
FREDRICKSON, A. G. 1964 *Principles and Applications of Rheology*. Prentice-Hall.
HINZE, J. O. 1959 *Turbulence*, p. 527. McGraw-Hill.
HOYT, J. W. 1972 *Trans. A.S.M.E., J. Basic Engng*, **D94**, 258.
JAKOWSKA, S. 1963 *New York Acad. Sci. Ann.* **106**, 458.
LING, S. C. 1963 *Trans. A.S.M.E., J. Heat Transfer*, **85**, 230.
ROSEN, M. W. & CORNFORD, N. E. 1971 *Nature*, **234**, 49.
RUDD, M. J. 1969 *Nature*, **224**, 587.
SCHLICHTING, H. 1968 *Boundary-Layer Theory*. McGraw-Hill.
VAN DRIEST, E. R. 1970 *J. Hydronautics*, **4**, 120.
VIRK, P. S. 1971 *J. Fluid Mech.* **45**, 417.
WALTERS, R. R. & WELLS, C. S. 1971 *J. Hydronautics*, **5**, 65.

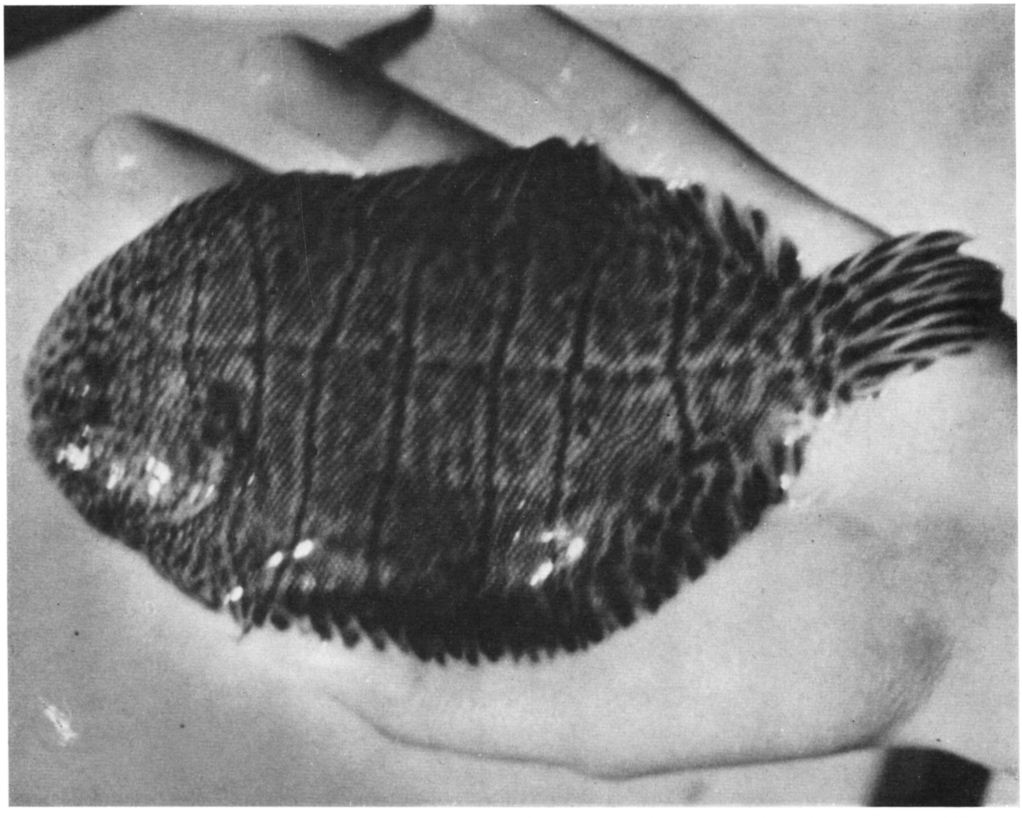

FIGURE 2. Hogchoker (*Trinectes maculatus*).